Microbiological Research 222 (2019) 52–59

Contents lists available at ScienceDirect

Microbiological Research

journal homepage: www.elsevier.com/locate/micres

Prediction of *in situ* metabolism of photobacteria in modified atmosphere packaged poultry meat using metatranscriptomic data

Linda Höll[1], Maik Hilgarth[1], Andreas J. Geissler, Jürgen Behr[2], Rudi F. Vogel*

Lehrstuhl für Technische Mikrobiologie, Technische Universität München, Freising, Germany

ARTICLE INFO

Keywords:
Meat spoilage
Modified atmosphere packaging
Matrix assisted laser desorption/ionization – time of flight
RNA sequencing
Photobacterium spp.

ABSTRACT

Modified atmosphere packaging (MAP) is widely used in food industry to extend the microbiological shelf life of meat. Common CO_2-containing gas atmospheres for poultry meat packaging are either nearly O_2-free or high O_2 MAPs. In this work, we compared spoilage microbiota of skinless chicken breast in CO_2/O_2 (30/70%) and CO_2/N_2 (30/70%) MAP, which are culturable with conventional methods and identified isolates by MALDI-TOF MS. These data were compared to metatranscriptome sequencing enabling a culture-independent overview on the composition of microbiota at species level. While typical MAP meat spoilers were confirmed in the transcriptomic approach, we also found high numbers of transcripts mapping to *Photobacterium* spp. sequences in these samples. As photobacteria were recently shown to occur in different MAP and vacuum packaged meats, we used the respective part of the metatranscriptomic data for prediction of *Photobacterium* spp. major metabolic routes *in situ*, upon growth in MAP poultry meat. It is predicted that they employ similar metabolism in both atmospheres: In the lack of carbohydrates upon meat spoilage, the pyruvate pool is filled via glycerol originating from lipolysis and amino acid conversions. From the pyruvate pool, gluconeogenesis is fed enabling cell wall biosynthesis and growth as well as catabolism to lactate and other metabolites, or anaplerosis towards the citric acid cycle. Production is predicted of several biogenic amines including tyramine and cadaverine, enabling generation of proton motive force. Taken together, photobacteria express metabolic pathways upon growth on meat, which should lead to compounds overlapping with those of known potent meat spoilers.

1. Introduction

Poultry meats are known to have a high initial contamination level and thus represent a highly perishable product, even under cold storage conditions (Vihavainen and Björkroth, 2010; Meredith et al., 2014; Rouger et al., 2017). Therefore, poultry meat is often packaged in CO_2/N_2 modified atmosphere, since CO_2 is an efficient inhibitor for meat spoilage bacteria, and retaining oxymyoglobin is not relevant in white meat (Sante et al., 1994; McKee, 2007). Still, some producers use high concentrations of oxygen in their packages, empirically achieving similar shelf lives (Rossaint et al., 2015). Höll et al. (2016) have shown that CO_2/O_2 packaging may also be advantageous, since it induces a change in the spoilage microbiota from predominant *Carnobacterium* (*C.*) spp., *Serratia* spp. and (potentially pathogenic) *Yersinia* spp. (in CO_2/N_2 MAP) to *Brochothrix* (*B.*) *thermosphacta*, *Carnobacterium* spp. and different *Pseudomonas* (*P.*) spp.

In order to get a conclusive overview of the major known spoilage bacteria on meat, most common methods used in laboratory routine control are culture-dependent using (non-) selective agars and incubation at 25–30 °C. However, there is a risk to let nutritionally fastidious and namely psychrophilic or psychrotrophic bacteria e.g. photobacteria unnoticed using these common routine methods. *Photobacterium* (*Ph.*) *phosphoreum* is a well-known light-organ symbiont of several fish species isolated from deep-sea marine environments (Hendrie et al., 1970) and also considered as typical member of the spoilage microbiota of seafood (Dalgaard et al., 1993, 1997). *Ph. phosphoreum* from this habitat are psychrophilic or psychrotrophic, NaCl requiring and nutritionally fastidious indicating that standard routine methods are not applicable for its detection (Dalgaard et al., 1997). Although photobacteria are known spoilers of seafood, their presence on meat and contribution to spoilage have been rarely reported in the past. Recently, employing culture-independent methods, abundance of photobacterial sequences

* Corresponding author at: Technische Universität München, Lehrstuhl für Technische Mikrobiologie, Gregor-Mendel-Straße 4, 85354 Freising, Germany.
E-mail addresses: linda.hoell@wzw.tum.de (L. Höll), maik.hilgarth@wzw.tum.de (M. Hilgarth), a-geissler@hotmail.com (A.J. Geissler), j.behr.leibniz-lsb@tum.de (J. Behr), rudi.vogel@wzw.tum.de (R.F. Vogel).
[1] Joint first authorship for equal contribution.
[2] Current address: Leibniz-Institut für Lebensmittel-Systembiologie an der Technischen Universität München, Freising, Germany.

https://doi.org/10.1016/j.micres.2019.03.002
Received 16 November 2018; Received in revised form 22 February 2019; Accepted 7 March 2019
Available online 08 March 2019
0944-5013/

on (minced) beef (Pennacchia et al., 2011; Stoops et al., 2015) and pork (Nieminen et al., 2016) has been demonstrated. Furthermore, an adapted isolation procedure was developed by Hilgarth et al. (2018a), who demonstrated frequent abundance of multiple *Photobacterium* species in relevant quantities on different MAP meats. *Ph. phosphoreum*, *Ph. iliopiscarium* and *Ph. carnosum* were found in 53% (8/15) of chicken samples, 22% (2/9) of pork samples, 100% (2/2) of beef samples, and on MAP salmon. *Ph. carnosum* sp. nov. was described as an isolate from meat (Hilgarth et al., 2018b), which was present in some of these samples. Given the common abundance on different meats and the previously demonstrated and acknowledged capability to spoil seafoods, a contribution of *Photobacterium* spp. to meat spoilage is probable. Still, the *in situ* metabolism of photobacteria growing on meat upon modified atmosphere packaging remains unknown.

In addition to culture-dependent routine analysis, an emerging trend in recent studies is the evaluation of microbial diversity by culture-independent high throughput sequencing of partial 16S rRNA gene amplicons of variable regions. While this technique has been used in environmental and intestinal studies (Lazarevic et al., 2009; Sáenz de Miera et al., 2014), other studies also employed this technique during salami fermentation (Greppi et al., 2015; Polka et al., 2015) or in water kefir (Gulitz et al., 2013) to demonstrate the abundance of unexpected and uncultured bacteria. Furthermore, the contamination routes of the spoiling microbiome on poultry meat have been previously analyzed by amplicon sequencing (Oakley et al., 2013; Rouger et al., 2017). However, this technique is mainly limited by the poor phylogenetic resolution on family or genera level, caused by limited length of sequence reads, which to date barely allow affiliation at species level. The emerging use of full-length 16S rRNA amplicon sequencing can only partially solve this issue because the 16S rRNA is not useful as a sole distinctive phylogenetic marker in many taxa. In contrast to 16S rRNA amplicon sequencing, metatranscriptomics delivers confirmation of species identification, as it can be considered as unbeatably broad "multi locus sequencing" approach. Furthermore, it also enables the *in silico* prediction of bacterial metabolism of specific spoilers taking place *in situ*. Most studies deal with the transcriptome analysis of only one specific strain, while others use the information of RNA sequencing for the assessment of the microbial diversity as described before (De Filippis et al., 2013; Andreevskaya et al., 2015). However, Jiang et al. (2016) used metatranscriptomic analysis for taxonomic and functional analysis of different microbiomes thus providing insight into contributions of different taxa to biochemical pathways.

This work aimed to generate a comprehensive overview on the microbiota development in CO_2/O_2 and CO_2/N_2 MAP skinless chicken breast. Strengths and limits of MALDI-TOF MS identification of cultured isolates to culture-independent metatranscriptomics should be delineated. In this proof of concept study, we used metatranscriptomic data to enable prediction and first insights into metabolic pathways, which are expressed in photobacteria upon growth on MAP poultry meat.

2. Materials and methods

2.1. Samples and packaging

One batch of skinless chicken breast was obtained from a local retailer at the second day after slaughtering. Samples were originally packaged with three to four pieces of meat in a CO_2/O_2 MAP with about 80% O_2 and 20% CO_2 and the minimum shelf life (MSL, the so-called use-by date) was specified with 8 days beginning with slaughtering (according to the producer). Directly after obtaining the samples, half of the breast filets were re-packed with 70% O_2 and 30% CO_2 (3 packages à 3 pieces, O_2-A/B/C), while the other half were re-packed with 70% N_2 and 30% CO_2 (3 packages à 3 pieces, N_2-A/B/C). All packages were stored at recommended 4 °C until use-by date. Then, packages were opened and samples for determination of total viable count and identification of the microbiota were taken. Additionally, RNA was extracted from the surface as described in 2.4.

2.2. Total viable count

For microbiological analysis, samples were taken aseptically from every breast filet and handled as described before by Höll et al. (2016). Microbiota was cultivated on brain-heart infusion agar for 48 h at 25 °C.

2.3. MALDI-TOF MS analysis

For determination of the microbiota composition by MALDI-TOF MS, a maximum of 96 single colonies (capacity of one 96 steel MALDI target) were picked for each sample. Methods were used as described by Höll et al. (2016). The raw data were processed as described in detail by Usbeck et al. (2013) and Kern et al. (2013).

2.4. RNA extraction

Chicken breasts out of each package were washed with 5 ml RNAprotect® bacteria reagent each. The suspension was used again for a second washing step and collected. For cell lysis, the suspension was mixed with DEPC-treated TE-buffer, containing 50 mg ml^{-1} lysozyme and 20 mg ml^{-1} proteinase K, and incubated for 1 h at 37 °C. The RNA was isolated, with some modifications, according to the suppliers' instructions in the RNAprotect® Bacteria Reagent Handbook (Protocol 5 and 7) using the RNeasy Mini kit (Qiagen GmbH, Hilden, Germany). Additionally, on-column DNase digestion using the RNase-Free-DNase Set (Qiagen GmbH, Hilden, Germany) was performed. The RNA was eluted in two steps with RNase-free water. Quality and quantity of isolated RNA was checked using NanoDrop 1000 spectrometer (Peqlab Biotechnolgie, Erlangen, Germany).

2.5. RNA sequencing and bioinformatics

RNA samples were sent to GATC Biotech (Konstanz, Germany) for transcriptome analysis. After rRNA depletion, mRNA was fragmented and cDNA libraries were constructed. The samples were sequenced (2 × 125 bp) via Illumina HiSeq2500. Bowtie 2 version 2.2.9 (Langmead and Salzberg, 2012), running with default mode settings (search for multiple alignments; report the best one; randomized), was used to map the generated paired-end reads on reference genomes (see following paragraph). The generated output files in SAM format (sequence alignment/map) were sorted and filtered using SAMtools (Li et al., 2009) and converted to BAM files (binary alignment/map).

Although a depletion of rRNA was conducted in order to enrich mRNA, the number of rRNA sequences was still high enough to employ a Bowtie 2 mapping in default mode to NCBI 16S database allowing selection of genomes as transcriptome reference. First, a genome selection (genome selection 1, Fig. S1 step 1 and 2) was used consisting of all available NCBI genomes (two genomes per species, if more than two were available, complete was preferred over chromosome and contig/scaffold assembly level) of those organisms, which were found to have at least five paired end properly paired reads to the NCBI 16S database (https://www.ncbi.nlm.nih.gov/bioproject/, Bioproject PRJNA33175). In a second approach, an enhanced genome selection was used for further alignments. Genome selection 2 (Tab. S1 and Fig. S1 step 3) consisted of genome selection 1 plus human and *Gallus gallus* for contamination, as well as about 300 genomes of other organisms of various genera, which were chosen based on a pre-experimental mapping with previous RNA-data (two genomes per species; preference regarding assembly level see genome selection 1). Genome selection 2 was the basis for the analysis of the microbiota distribution and gene expression. For the alignment on gene level, all NCBI annotated genomes (open reading frames, ORFs) from organisms with more than 1000 paired end properly paired reads were selected (Tab. S2 and Fig. S1, step 4).

Part of these genome selections were also five spoilage-related bacteria, which were isolated during the spoilage of poultry meat, as part of this study. Whole genome sequencing was done for two strains of *B. thermosphacta* (TMW 2.1564, TMW 2.1572), one strain of *C. divergens* (TMW 2.1579), one strain of *C. maltaromaticum* (TWM 2.1581), as well as one strain of *Pseudomonas* sp. (TMW 2.1634). Subsequently, genomes were submitted to the NCBI Prokaryotic Genome Annotation Pipeline for annotation (bioproject PRJNA336488 with the biosamples SAMN05511621, SAMN05511622, SAMN05511623, SAMN05511624 and SAMN05511625).The KEGG Automated Annotation Server (KAAS) (Moriya et al., 2007) was used to assign the relevant ORFs of selected species to a KEGG Orthology (KO) (Kanehisa and Goto, 2000) for metabolic analyses. For functional assignment, genes with the 10% highest gene counts (upper 10% ORFs) of the relevant species in every sample were selected (Fig. S1, step 5) and categorized using the cluster of orthologous groups (COG) categories (Galperin et al., 2015) applying WebMGA (http://weizhong-lab.ucsd.edu/metagenomic-analysis/) of Wu et al. (2011). For normalization of gene counts and the differential gene expression analysis, the R package DESeq (Anders and Huber, 2010) was used. Genes were considered as significantly differentially expressed with a p-value of < 0.05.

3. Results

3.1. Microbiota composition in CO_2/O_2 and CO_2/N_2 MAP

Table 1 shows the culturable microbiota after 8 days of storage at the use-by date. The different MA compositions (CO_2/O_2 and CO_2/N_2) had no influence on the spoilage-associated microbiota. In both atmospheres, the CFU were about 5.7×10^7 CFU cm^{-2} and the community composition was very similar.

The microbiota composition was identified by MALDI-TOF MS as well as by analysis of RNA sequences from the metatranscriptomic approach. The relative species abundance of the culture-dependent identification is shown in Fig. 1A. All triplicates (A, B, C) of chicken samples packed in CO_2/O_2 MAP (three bars on the left) were dominated by *B. thermosphacta*, followed by *Carnobacterium* spp., among which *C. divergens* was more abundant than *C. maltaromaticum*. In addition, *Lactobacillus* spp. and *L. piscium* were detected in significant numbers and low numbers of *Pseudomonas* spp. (A) and *Serratia* spp. (C) isolates could be identified in two samples. In samples packed in CO_2/N_2 MAP (three bars on the right) *B. thermosphacta* was less abundant. Two samples (A, C) were dominated by *Brochothrix* (52%), while the third sample was dominated by LAB, mainly *Carnobacterium* spp. (B, 32%). In contrast to the CO_2/O_2 atmosphere, *Serratia* spp. was detected in all three samples stored under anoxic conditions. Additionally, *L. piscium* had higher abundance under these atmospheric conditions.

The transcriptomic raw datasets generated and analyzed during the current study are deposited in the European Nucleotide Archive of the EMBL-EBI. The study accession number is PRJEB26438. Mapping statistics of the respective database selection are shown in Tab. S5. The sample accession numbers are ERS2433918-29. The results of the culture-independent sequences obtained by metatranscriptomic analysis are shown in Fig. 1B for storage in CO_2/O_2 (three bars left) and CO_2/N_2 MAP (three bars right). The results were calculated from the proper paired best hit alignments [%] of metatranscriptomic data with genome selection 2 (Tab. S1). All genera are depicted, which represent at least 1% of the proper paired best hit alignments of the respective sample.

Table 1
Culturable bacterial load of the samples for the transcriptomic analysis after 8 days of storage at 4 °C.

Sample	CFU cm^{-2}	Standard deviation
CO_2/O_2		
A	5.43E + 07	1.49E + 07
B	5.37E + 07	9.14E + 06
C	6.26E + 07	1.79E + 07
CO_2/N_2		
A	5.43E + 07	1.88E + 07
B	6.54E + 07	8.23E + 06
C	5.37E + 07	3.77E + 06

The results for storage in CO_2/O_2 MAP were not consistent. One sample (A) was dominated by *Photobacterium* (*Ph.*) spp., while the other samples (B, C) were dominated by *B. thermosphacta* and *Carnobacterium* spp., which were also dominant within the cultured microbiota. The most abundant species according to metatranscriptome mapping was *Ph. phosphoreum* with 40.8%. Additionally, small amounts of chicken (*Gallus gallus*) (CO_2/O_2: 2.8–8.27%, CO_2/N_2: 2.4–3.6%) and human RNA/cDNA (CO_2/O_2: 1.2–1.6%, CO_2/N_2: 1.4–1.5%) were isolated from the samples and could not be removed by rRNA depletion. Therefore, they were also part of the identified "microbiota". *Pseudomonas* spp. were either not detected at all or occurred or in numbers of $\leq 0.1\%$.

Samples stored in CO_2/O_2 MAP were all dominated by *Photobacterium* spp. as in one sample packed in CO_2/N_2 (O2_A). The dominant species in the culture independent analysis was again *Ph. phosphoreum*, besides accessory *B. thermosphacta* and *Carnobacterium* spp., which were identified as dominant species within the cultured microbiota.

3.2. Gene expression analysis of Photobacterium spp. and metabolic prediction

Metatranscriptomic datasets exhibit not only taxonomic, but also functional signatures. In this communication, we focus on the transcriptomic analysis of uncultured *Ph. iliopiscarium* and *Ph. phosphoreum* for predictions on their *in situ* metabolism. The basis for gene annotation were 10 NCBI-annotated photobacteria genomes shown in Tab. S2. Tables with locus tags and gene counts were sorted regarding the different species and samples (Tab. S3). After evaluating the frequency distribution of gene counts in dependence on the mean values, the upper 10% genes (Fig. S2) of every species were selected for further analysis. For gene expression analysis of *Ph. phosphoreum*, we included all relevant samples (O2_A, N2_A, N2_B, N2_C) in order to gain results on possible metabolic differences in CO_2/O_2 versus CO_2/N_2 MAP.

Photobacterium spp. could be detected in all CO_2/N_2 MAP and in one CO_2/O_2 sample with high abundancies. The functional analysis in COG categories for *Ph. iliopiscarium* and *Ph. phosphoreum* is shown in Fig. S3. Translation and ribosomal structures were the main parts found in both atmospheres, followed by proteins related to energy production/conversion and carbohydrate transport/metabolism. Regarding the classification in COG categories, only minor differences could be found between both species.

Also, transcript patterns in both atmospheres were similar for *Ph. phosphoreum* and *Ph. iliopiscarium*. Proteins with the highest gene counts, are shown (independently from the atmosphere) for *Ph. phosphoreum* in Tab. S3, and for *Ph. iliopiscarium* (in CO_2/N_2 atmosphere) in Tab. S4. According to the bioinformatic prediction, *Ph. phosphoreum* was more abundant, and numbers of transcripts mapping to this species were in statistically relevant numbers in both atmospheres. Therefore, the metabolic prediction was subsequently focused on that species as major representative for the overlapping metabolism of all photobacteria in the samples. Additionally, a differential gene expression analysis was conducted for *Ph. phosphoreum*. Fig. S4 shows the $\log_2$ fold changes for the upper 10% normalized gene counts in CO_2/O_2 and CO_2/N_2 MAP. The maximum log fold change in CO_2/O_2 MAP was 1.70, while in CO_2/N_2 MAP the values reached a minimum of -2.75. Table 2 shows the significant differentially expressed genes ($p < 0.05$) in both atmospheres. The gene highest upregulated in CO_2/O_2 MAP was the NADP-dependent oxidoreductase, a domain of different aldo-keto reductases, e.g. aldehyde reductase, aldose reductase, or xylose reductase.

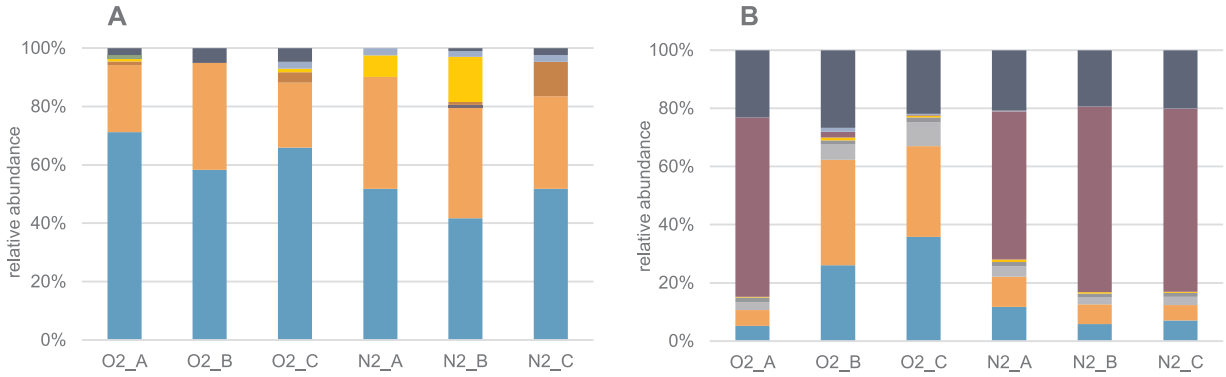

Fig. 1. A Microbiota distribution of three independent samples (A, B, C) in CO_2/O_2 (O2) and CO_2/N_2 MAP (N2), identified by MALDI-TOF MS. The samples were taken on the day of minimum shelf life after 8 days of storage at 4 °C. All species, which were identified > 1%, are depicted. **B** Microbiota distribution of three independent samples (A, B, C) in CO_2/O_2 (O2) and CO_2/N_2 MAP (N2), calculated from the proper paired best hit alignments [%] of metatranscriptomic data. The samples were taken on the day of minimum shelf life after 8 days of storage at 4 °C. All bacteria genera are depicted which represent ≥1% of the proper paired best hit alignments. *B. thermosphacta* (●), *Carnobacterium* spp. (●), *Gallus gallus* (●), Human (●), *H. alvei* (●), *Lactobacillus* spp. (●), *L. piscium* (●), *Photobacterium* spp. (●), *Serratia* spp. (●), others (●), *Pseudomonas* spp. (●), mixed microbiota/others (●).

Also, factors for translation and transcription were upregulated. No genes encoding enzymes of the predicted metabolism pathways (Fig. 2) were detected as significantly differentially expressed as indicated by a p value > 0.05, suggesting a similar metabolism on poultry meat independent of the modified atmosphere (O_2/CO_2, N_2/CO_2) used.

Besides ribosomal genes associated with translation and transcription, genes for central metabolism represented the major part of total sequences. An overview of the predicted *in situ* carbon metabolism of *Ph. phosphoreum* on poultry meat is shown in Fig. 2. The highest gene counts were found for formate acetyltransferase, an enzyme of the anaerobic pyruvate metabolism, which catalyzes the conversion of pyruvate to acetyl-CoA. *Ph. phosphoreum* is also able to produce ethanol, acetate, formate, lactate and acetoin from pyruvate. (*Ph. iliopiscarium* is missing acetolactate decarboxylase). However, pyruvate can also originate from citrate or glycerol present as constituent of lipids in the meat. Additionally, low numbers of transcripts (< 100 / sample) were also found for the production of pyruvate by transamination of amino acids e.g. alanine (alanine-glyoxylate aminotransferase).

Furthermore, glycolysis, the pentose phosphate pathway, (cf. Fig. 2) as well as the citrate cycle were complete and expressed.

Ph. phosphoreum can also use fat, namely triglycerides, as energy source upon growth. Triglycerides can be degraded to fatty acids and a glycerol moiety, which is then metabolized to dihydroxyacetonephosphate and used in pyruvate metabolism (cf. Fig. 2).

Additionally, *Ph. phosphoreum* expresses genes encoding several decarboxylases upon growth in both MAP atmospheres, which facilitate formation of biogenic amines from amino acids. Transcripts of ornithine, lysine, arginine, tyrosine and glutamate decarboxylases were detected (> 50 gene counts per sample) leading to the formation of putrescine, cadaverine, agmatine, tyramine and GABA, respectively. Transcripts of histidine decarboxylase were not detected (< 50 gene counts per sample) and phenylalanine decarboxylase is not present in the genome.

Ph. phosphoreum expressed also genes necessary to establish a functional aerobic and anaerobic respiratory chain using oxygen or alternative electron acceptors, respectively. Transcripts (> 100 gene counts per sample) were found for TMAO reductase, nitrate reductase and fumarate reductase. Genes encoding ferredoxin oxidoreductase,

Table 2
Annotation and function of genes detected as statistically significant differentially expressed ($p < 0.05$) in CO_2/O_2 MAP poultry meat samples (positive log2 fold change) and in CO_2/N_2 MAP poultry meat samples (negative log2 fold change) in dependence of the upper 10% of the mean values of normalized counts and with a log2 fold change ≤ -1.0 and ≥ 1.0.

Annotation	COG category	Base mean	Log_2 fold change	p value
NADP-dependent oxidoreductase	general function predicted only	2987.1	1.7	9.62E-06
S-(hydroxymethyl)-glutathione synthase	coenzymes/ translation	1606.05	1.43	3.32E-05
glutathione S-transferase	postransl. modification	1587.01	1.43	2.57E-15
cold-shock protein	stress response	3421.39	1.32	2.40E-03
glutaminase	amino acid metabolism	9239.83	1.29	5.75E-05
alkene reductase		1667.85	1.08	3.81E-08
molecular chaperone DnaJ	posttranslat. modification	2168.79	1.04	7.74E-04
hypothetical protein		3147.89	1.04	1.99E-04
ATP-dependent chaperone ClpB	posttranslat. modification	19900.17	1.03	1.95E-03
hypothetical protein		2352.36	1.03	3.17E-03
S-formylglutathione hydrolase	posttranslat. modification	1670.94	1.02	2.67E-04
NADH:ubiquinone reductase (Na(+)-transporting) subunit B	energy production	2811.34	−1.02	4.25E-03
ribosomal protein L11 methyltransferase	translation	1808.28	−1.03	1.96E-06
adenylosuccinate synthetase	nucleotide metabolism	9127.74	−1.08	9.34E-03
phosphatase/phosphotransferase	carbohydrate metabolism	3516.16	−1.14	5.25E-06
NADH:ubiquinone reductase (Na(+)-transporting) subunit A	energy production	4461.04	−1.18	1.95E-03
effector protein		1757.16	−1.22	2.83E-05
hypothetical protein		4631.28	−1.39	1.77E-09
DNA starvation/stationary phase protection protein	ion transport	1804.91	−1.5	4.04E-07
MFS transporter	carbohydrate metabolism	2621.58	−1.63	1.92E-02
hydrogenase 4 subunit B	energy production	1868.93	−1.76	6.96E-13
nucleoside transporter NupC	nucleotide metabolism	1684.69	−2.75	2.65E-02

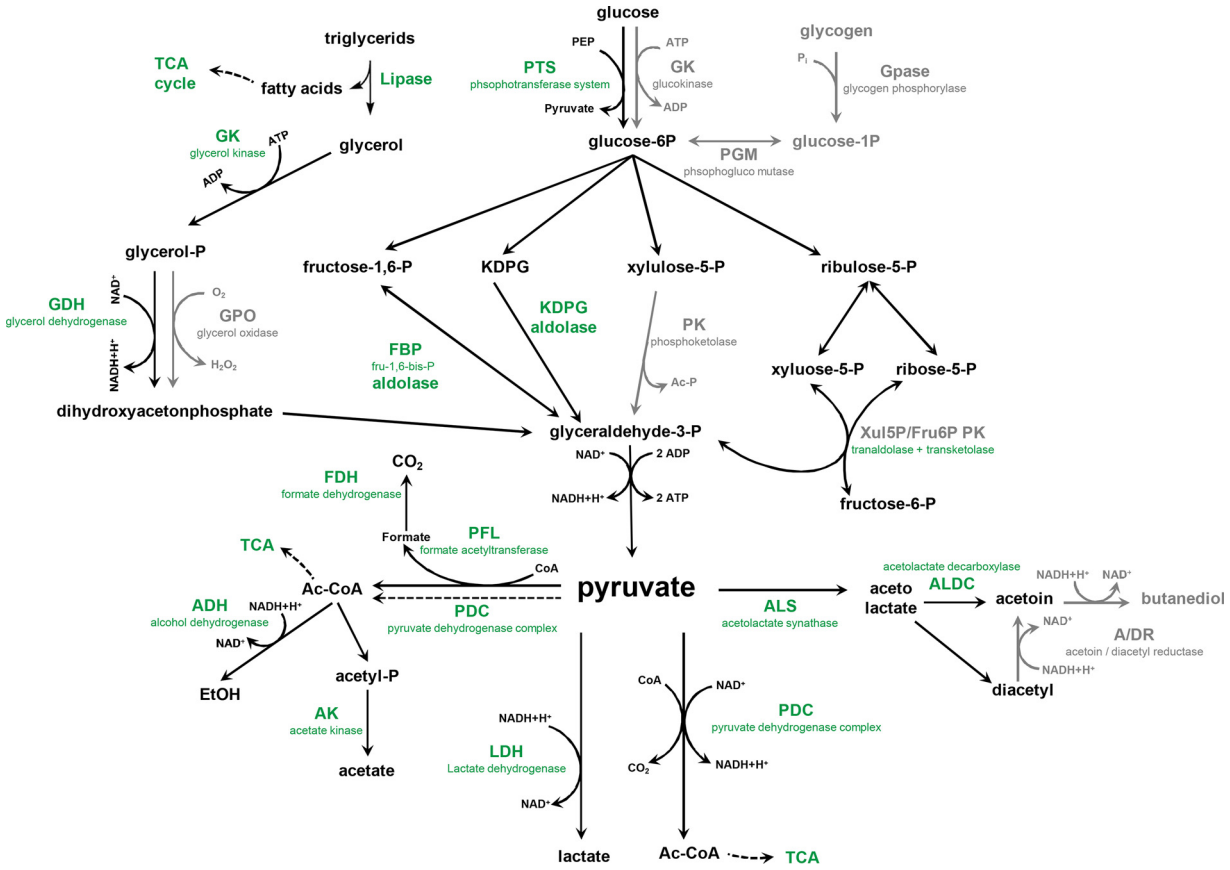

Fig. 2. Predicted pathway of carbon metabolism of *Ph. phosphoreum.* Glucose is metabolized to glucose-6-phosphate and degraded to gylcerinealdehyde-3-phophate in several pathways: glycolysis, Entner-Doudoroff-, phosphoketolase and pentose phosphate pathway (from left to right) following downstream fermentative and respiratory pyruvate fates. The green color indicates the presence of genes in the genome and the detection of transcripts (> 50 gene counts per sample), while the grey color indicates, that genes are not part of the genome.

and sulfate adenyltransferase, sulfate kinase and sulfite reductase were present in the genome, but transcripts were detected only as < 50 gene counts per sample.

4. Discussion

4.1. Comparison of culture-dependent and culture-independent approach

In this work, microbiota analyses performed by culture-dependent MALDI-TOF MS were compared with culture-independent metatranscriptomic analyses with regard of identification of all relevant spoilage bacteria, handling and expenditure of time. This study supports the employment of a combined approach using culture-dependent and -independent approaches to achieve a comprehensive overview. As demonstrated in this study, photobacteria cannot be isolated with conventional/routine methods, and require a specific isolation procedure for recovery (Hilgarth et al., 2018a). Furthermore, analysis of transcripts from photobacteria in the metatranscriptomic dataset allowed predictions of their *in situ* metabolism on MAP meats, which was previously unknown.

With the establishment of a detailed database, the MALDI-TOF MS technique proved as a powerful tool to dissect microbiota dynamics upon spoilage. Höll et al. (2016) demonstrated the discriminatory power of MALDI-TOF MS along the identification and growth dynamics of meat spoiling bacteria employing 25 °C and BHI for recovery of bacteria. This approach allowed isolation of typical representatives of the autochthonous microbiota according to the different meat types (Doulgeraki et al., 2012). A demonstrated limit results from the cultivation temperature of 25 °C, because some obligate psychrophiles and fastidious organisms e.g. photobacteria can not be isolated from cold stored meats. The validity of this limit is demonstrated in our study by the use of alternative, culture-independent sequencing technology.

Employing a multilayered mapping workflow (Fig. S1), we were able to map more than 90% of transcripts to our final genome selection enabling detailed transcriptomic analysis and affiliation of transcripts to bacteria at species level. This way, we could identify *Ph. phosphoreum* and *Ph. iliopiscarium* as major representatives of photobacteria. The relative numbers of *Photobacterium* rRNA sequences in the samples as compared to other spoilers found as major players in culture-dependent and culture independent approaches were high and sometimes higher than those of *Carnobacterium* and *Brochothrix* demonstrating their predominance within the microbiota growing on MAP chicken meat. The photobacteria sequences were found in samples packed in both modified atmospheres, however, only in one of three CO_2/O_2 samples. This suggests that their lifestyle enables aerobic as well as anaerobic growth in presence of CO_2 and the choice of atmosphere has limited if any effect on their growth. The absence of differential gene expression as a result of growth in different MAP suggests a similar metabolism independently of the MAP applied and corroborates this víew. The fact that we did not find photobacteria sequences in every single sample derived from one initial batch, suggests that initial contamination with these organisms is very low, and may therefore vary even between different pieces of meat. In practical terms, this means that their entry into the food production chain has to be identified and minimized.

4.2. Photobacteria as dominant constituents of the spoilage microbiota

Photobacteria are typical members of the spoilage microbiota of

seafood (Dalgaard et al., 1993, 1997), but have also been described as sporadic members of meat spoilage microbiota of beef and pork (Pennacchia et al., 2011; Stoops et al., 2015; Nieminen et al., 2016). Employing conventional culture-dependent methods, it is rather unlikely to recover photobacteria, e.g. *Ph. phosphoreum*, since it is psychrophilic (preferential growth at 15 °C), NaCl requiring and nutritionally fastidious. Therefore, spread plating methods on standard media e.g. plate count agar with incubation temperatures between 23–25 °C or higher are not useful for its detection (Dalgaard et al., 1997; Nieminen et al., 2016). A recent comparative isolation approach demonstrated that an targeted selective isolation procedure is required to recover photobacteria from different MAP meats (Hilgarth et al., 2018a). These findings are corroborated in our study, suggesting a combination of culture-dependent with a culture-independent approach for community analysis in order to complement the respective limitations. In this proof of concept study, transcriptomic analysis of photobacteria growing on MAP meat in a natural (non-inoculated) sample delivered a realistic prediction on their *in situ* metabolism in the presence of the other consortium members and an impression why meat serves as an ecological niche for these bacteria by using part of the metatranscriptomic data set. Within the transcripts mapping to members of photobacteria, *Ph. phosphoreum* represented the most abundant species in regard to percentages of mapped transcripts, followed by *Ph. iliopiscarium* and minor abundant *Ph. carnosum*. For metabolic prediction, we have therefore focused on *Ph. phosphoreum*. The average read length of these transcripts was 125 bp, and the mapping allowed a mismatch of 2 bp within 100 bp. As e.g. *Ph. iliopiscarium* and *Ph. carnosum* are very closely related, it can be assumed that part of the transcripts mapping to *Ph. phosphoreum* also mapped to these species. This view is supported by the similarity of gene expression within COG categories for *Ph. phosphoreum* and *Ph. iliopiscarium*. Therefore, the major metabolic predictions made for *Ph. phosphoreum* can be seen as representative for *Photobacterium*, with some demonstrated differences between the different species.

4.3. Predictive glycolytic metabolism of Ph. phosphoreum

Generally, *Ph. phosphoreum* is described as a Gram-negative, facultative anaerobic bacterium, fermenting glucose to gas/and or acid (Hendrie et al., 1970). This was also shown in our transcriptome analyses. *Ph. phosphoreum* expressed all genes for glycolysis, i.e. catabolism of glycogen, glucose and ribose to pyruvate. This might suggest that despite any assumption on limited sugar availability at the end of shelf life and onset of spoilage, there is still sugar available. Although glucose levels are decreasing during storage, the actual availability of glucose in poultry meat also at late stages of storage has been previously demonstrated (Kakouri and Nychas, 1994; Nychas and Tassou, 1997). However, most reactions of the glycolytic pathway are reversible, and annotation as well as *in silico* metabolic pathway databases do not reveal the specific direction of a reaction and thus, for many enzymes, do not distinguish between anabolic and catabolic reactions. The more likely interpretation therefore is that in the lack of sugars, gluconeogenesis from pyruvate is active, providing components for cell wall biosynthesis and increase of biomass. At the same time, the photobacteria in MAP chicken should be able to produce ethanol, acetate, formate, and lactate from pyruvate. The highest number of transcripts was detected for formate acetyltransferase, an enzyme related to anaerobic pyruvate metabolism, which catalyzes the conversion of pyruvate to acetyl-CoA. The pyruvate appears to originate from the glycerol moiety of lipids in the meat or from the desamination of amino acids like alanine. Indeed, transcripts were found for all relevant enzymes participating in the degradation of triglycerides-derived glycerol to dihydroxyacetone phosphate and thus feeding pyruvate conversion reactions. The impact of glucose limitation on gene expression pattern and the upregulation of genes involved in the amino acid or lipid catabolism has been previously demonstrated for meat spoiling *P. putida* (Mohareb et al., 2015).

4.4. Predicted respiratory alternative electron acceptors upon growth in MAP

Since *Ph. phosphoreum* is known as a typical member of the spoilage microbiota of fish products, many sensorial negative effects were described for this type of food. The spoilage of raw fish and fish products by *Ph. phosphoreum* is associated with the production of trimethylamine, other biogenic amines and acetic acid (Jorgensen et al., 2000; Dalgaard et al., 2006; Macé et al., 2013). It is likely that some of these are also relevant for meat. Trimethylamine is a very strong off-odor with a fishy perception and is produced by the oxidation of trimethylamine N-oxide, serving as alternative electron acceptor during anaerobic respiration also in *Ph. phosphoreum* (Proctor and Gunsalus, 2000). Upon growth on poultry meat, transcripts were found for trimethylamine N-oxide reductase, as well as for other alternative electron acceptors, namely nitrate, iron (III), fumarate, sulfate and sulfite. However, it remains speculative whether the respective conversion reactions are performed in regard to their availability or the expression of these genes rather follows a general regulatory response triggered by the CO_2. As a result of inhibition of aerobic respiration or the lack of oxygen in the modified atmosphere, the photobacteria may just induce expression of genes related to anaerobic respiration in general. This view seems likely, because in poultry meat, amounts of nitrate and trimethylamine N-oxide are very low or even not available at all (Mitchell et al., 2002; Iammarino and Di Taranto, 2012).

4.5. Predicted biogenic amine production of Ph. phosphoreum on poultry meat

Another common factor indicating spoilage of foods is the formation of biogenic amines, which also harbor risks to human health upon consumption and can lead to food poisoning. They are mainly produced by LAB and *Enterobacterales*, and have been described for wines, vegetables, cheese, meat and also fish (Santos, 1996; Durlu-Özkaya et al., 2001; Hammes and Hertel, 2006). Still, they have also been observed in combination with high numbers of *Ph. phosphoreum* (Jorgensen et al., 2000; Naila et al., 2010). A study by Balamatsia et al. (2006) has investigated the formation of biogenic amines in chicken breast during storage under aerobic and MAP conditions at 4 °C and proposed a biogenic amines index (values between 96 and 101 mg kg^{-1} indicate freshness), calculated from the sum of putrescine, cadaverine and tyramine, to graduate the quality of poultry meat. Within all members of meat-associated microbiota we could identify, *Ph. phosphoreum* was the species with the highest diversity of predicted biogenic amine production. Results of the gene expression analysis predicted the production of putrescine, cadaverine, agmatine, tyramine and GABA. Since high numbers of transcripts (3000–6000) of antiporters for histidine/histamine, putrescin/ornithine and lysine/cadaverine were detected, it is likely that they use these reactions for the generation of proton motive force, which may help to maintain assertiveness in the habitat (Molenaar et al., 1993; Fernandez and Zuniga, 2006). In comparison, only 200–500 transcripts were found for amino acid ABC transporters. The extensive conversion of amino acids to amines should enable the bacterium to keep up its preferential intracellular and micro-environmental pH and counteract any acidification caused by competing LAB or *Brochothrix*.

4.6. Conclusion

In conclusion, the detection of *Photobacterium* spp. in meats either requires a targeted culturing approach using specific media and conditions (Hilgarth et al., 2018a), or culture-independent analysis. This work demonstrates that sequencing techniques, namely metatranscriptomic analysis, can help to establish a more comprehensive

overview on microbiota and deliver targets for the adjustment of cultivation-based methods. In addition, predictions are possible on the *in situ* metabolism even of uncultured species. Taken together, this study demonstrated the importance of a complementary approach comprising cultivation-dependent as well as -independent techniques. By using part of the metatranscriptomic data set, we were able to predict the *in situ* metabolism of photobacteria growing on poultry meat, which appears to be independent of the MAP applied. The predicted metabolic pathways provide insight in their lifestyle in this habitat. Some of these pathways should lead to the formation of compounds, which overlap with those bacteria described as relevant for spoilage (Gram et al., 2002; Nychas et al., 2008; Doulgeraki et al., 2012). Indeed, the metatranscriptomic dataset obtained in this study also reveals overlap of the respective part of photobacterial metabolism with the respective predicted *in situ* metabolism of *Brochothrix* and *Carnobacterium*. Together with the fact that photobacteria are acknowledged as potent seafood spoilers and recent proof that multiple *Photobacterium* species are abundant in high numbers on different MAP meats, the *in situ* metabolism on MAP meat predicted in this study delivers evidence for the hitherto underestimated contribution of photobacteria to meat spoilage. These findings will impact on the interpretation of previous and forthcoming studies on meat spoilage.

Conflict of interest

The authors declare no conflict of interest.

Acknowledgements

Part this work was funded by the German Federal Ministry for Economic Affairs and Energy via the German Federation of Industrial Research Associations (AiF) and the Industry Association for Food Technology and Packaging (IVLV); project number AiF 17803 N.

Appendix A. Supplementary data

Supplementary material related to this article can be found, in the online version, at doi:https://doi.org/10.1016/j.micres.2019.03.002.

References

Anders, S., Huber, W., 2010. Differential expression analysis for sequence count data. Genome Biol. 11 (10), R106.

Andreevskaya, M., Johansson, P., Laine, P., Smolander, O.P., Sonck, M., Rahkila, R., Jaaskelainen, E., Paulin, L., Auvinen, P., Björkroth, J., 2015. Genome sequence and transcriptome analysis of meat-spoilage-associated lactic acid bacterium *Lactococcus piscium* MKFS47. Appl. Environ. Microbiol. 81 (11), 3800–3811.

Balamatsia, C.C., Paleologos, E.K., Kontominas, M.G., Savvaidis, I.N., 2006. Correlation between microbial flora, sensory changes and biogenic amines formation in fresh chicken meat stored aerobically or under modified atmosphere packaging at 4 °C: possible role of biogenic amines as spoilage indicators. Antonie Van Leeuwenhoek 89 (1), 9–17.

Dalgaard, P., Gram, L., Huss, H.H., 1993. Spoilage and shelf-life of cod fillets packed in vacuum or modified atmospheres. Int. J. Food Microbiol. 19 (4), 283–294.

Dalgaard, P., Mejholm, O., Christiansen, T.J., Huss, H.H., 1997. Importance of *Photobacterium phosphoreum* in relation to spoilage of modified atmosphere-packed fish products. Lett. Appl. Microbiol. 24 (5), 373–378.

Dalgaard, P., Madsen, H., Samieian, N., Emborg, J., 2006. Biogenic amine formation and microbial spoilage in chilled garfish (Belone belone belone)–effect of modified atmosphere packaging and previous frozen storage. J. Appl. Microbiol. 101 (1), 80–95.

De Filippis, F., La Storia, A., Villani, F., Ercolini, D., 2013. Exploring the sources of bacterial spoilers in beefsteaks by culture-independent high-throughput sequencing. PLoS One 8 (7), e70222.

Doulgeraki, A.I., Ercolini, D., Villani, F., Nychas, G.J., 2012. Spoilage microbiota associated to the storage of raw meat in different conditions. Int. J. Food Microbiol. 157 (2), 130–141.

Durlu-Özkaya, F., Ayhan, K., Vural, N., 2001. Biogenic amines produced by *Enterobacteriaceae* isolated from meat products. Meat Sci. 58 (2), 163–166.

Fernandez, M., Zuniga, M., 2006. Amino acid catabolic pathways of lactic acid bacteria. Crit. Rev. Microbiol. 32 (3), 155–183.

Galperin, M.Y., Makarova, K.S., Wolf, Y.I., Koonin, E.V., 2015. Expanded microbial genome coverage and improved protein family annotation in the COG database. Nucleic Acids Res. 43, D261–D269 Database issue.

Gram, L., Ravn, L., Rasch, M., Bruhn, J.B., Christensen, A.B., Givskov, M., 2002. Food spoilage – interactions between food spoilage bacteria. Int. J. Food Microbiol. 78 (1), 79–97.

Greppi, A., Ferrocino, I., La Storia, A., Rantsiou, K., Ercolini, D., Cocolin, L., 2015. Monitoring of the microbiota of fermented sausages by culture independent rRNA-based approaches. Int. J. Food Microbiol. 212, 67–75.

Gulitz, A., Stadie, J., Ehrmann, M.A., Ludwig, W., Vogel, R.F., 2013. Comparative phylobiomic analysis of the bacterial community of water kefir by 16S rRNA gene amplicon sequencing and ARDRA analysis. J. Appl. Microbiol. 114 (4), 1082–1091.

Hammes, W.P., Hertel, C., 2006. The Genera *Lactobacillus* and *Carnobacterium*. pp. 320–403.

Hendrie, M.S., Hodgkiss, W., Shewan, J.M., 1970. The identification, taxonomy and classification of luminous bacteria. J. Gen. Microbiol. 64 (2), 151–169.

Hilgarth, M., Fuertes-Pèrez, S., Ehrmann, M., Vogel, R., 2018a. An adapted isolation procedure reveals *Photobacterium* spp. as common spoilers on modified atmosphere packaged meats. Lett. Appl. Microbiol. 66 (4), 262–267.

Hilgarth, M., Fuertes-Pèrez, S., Ehrmann, M., Vogel, R., 2018b. *Photobacterium carnosum* sp. nov., isolated from spoiled modified atmosphere packaged poultry meat. Syst. Appl. Microbiol. 41 (1), 44–50.

Höll, L., Behr, J., Vogel, R.F., 2016. Identification and growth dynamics of meat spoilage microorganisms in modified atmosphere packaged poultry meat by MALDI-TOF MS. Food Microbiol. 60, 84–91.

Iammarino, M., Di Taranto, A., 2012. Nitrite and nitrate in fresh meats: a contribution to the estimation of admissible maximum limits to introduce in directive 95/2/EC. Int. J. Food Sci. Technol. 47 (9), 1852–1858.

Jiang, Y., Xiong, X., Danska, J., Parkinson, J., 2016. Metatranscriptomic analysis of diverse microbial communities reveals core metabolic pathways and microbiome-specific functionality. Microbiome 4, 2.

Jorgensen, L.V., Dalgaard, P., Huss, H.H., 2000. Multiple compound quality index for cold-smoked salmon (*Salmo salar*) developed by multivariate regression of biogenic amines and pH. J. Agric. Food Chem. 48 (6), 2448–2453.

Kakouri, A., Nychas, G., 1994. Storage of poultry meat under modified atmospheres or vacuum packs: possible role of microbial metabolites as indicator of spoilage. J. Appl. Microbiol. 76 (2), 163–172.

Kanehisa, M., Goto, S., 2000. KEGG: kyoto encyclopedia of genes and genomes. Nucleic Acids Res. 28 (1), 27–30.

Kern, C.C., Usbeck, J.C., Vogel, R.F., Behr, J., 2013. Optimization of matrix-assisted-laser-desorption-ionization-time-of-flight mass spectrometry for the identification of bacterial contaminants in beverages. J. Microbiol. Methods 93 (3), 185–191.

Langmead, B., Salzberg, S.L., 2012. Fast gapped-read alignment with Bowtie 2. Nat. Methods 9 (4), 357–359.

Lazarevic, V., Whiteson, K., Huse, S., Hernandez, D., Farinelli, L., Osteras, M., Schrenzel, J., Francois, P., 2009. Metagenomic study of the oral microbiota by Illumina high-throughput sequencing. J. Microbiol. Methods 79 (3), 266–271.

Li, H., Handsaker, B., Wysoker, A., Fennell, T., Ruan, J., Homer, N., Marth, G., Abecasis, G., Durbin, R., 2009. Genome project data processing S. The sequence alignment/map format and SAMtools. Bioinformatics 25 (16), 2078–2079.

Macé, S., Joffraud, J.-J., Cardinal, M., Malcheva, M., Cornet, J., Lalanne, V., Chevalier, F., Sérot, T., Pilet, M.-F., Dousset, X., 2013. Evaluation of the spoilage potential of bacteria isolated from spoiled raw salmon (*Salmo salar*) fillets stored under modified atmosphere packaging. Int. J. Food Microbiol. 160 (3), 227–238.

McKee, L., 2007. Microbiological and sensory properties of fresh and frozen poultry. In: Nollet, L.M.L. (Ed.), Handbook of Meat, Poultry and Seafood Quality. Blackwell Publishing, Ames, Iowa,USA.

Meredith, H., Valdramidis, V., Rotabakk, B.T., Sivertsvik, M., McDowell, D., Bolton, D.J., 2014. Effect of different modified atmospheric packaging (MAP) gaseous combinations on *Campylobacter* and the shelf-life of chilled poultry fillets. Food Microbiol. 44 (0), 196–203.

Mitchell, S., Zhang, A., Smith, R., 2002. Chemical and biological liberation of trimethylamine from foods. J. Food Anal. 15 (3), 277–282.

Mohareb, F., Iriondo, M., Doulgeraki, A.I., Van Hoek, A., Aarts, H., Cauchi, M., G-JE, Nychas, 2015. Identification of meat spoilage gene biomarkers in *Pseudomonas putida* using gene profiling. Food Control 57, 152–160.

Molenaar, D., Bosscher, J.S., ten Brink, B., Driessen, A.J., Konings, W.N., 1993. Generation of a proton motive force by histidine decarboxylation and electrogenic histidine/histamine antiport in *Lactobacillus buchneri*. J. Bacteriol. 175 (10), 2864–2870.

Moriya, Y., Itoh, M., Okuda, S., Yoshizawa, A.C., Kanehisa, M., 2007. KAAS: an automatic genome annotation and pathway reconstruction server. Nucleic Acids Res. 35, W182–W185 Web Server issue.

Naila, A., Flint, S., Fletcher, G., Bremer, P., Meerdink, G., 2010. Control of biogenic amines in food—existing and emerging approaches. J. Food Sci. 75 (7), R139–R150.

Nieminen, T.T., Dalgaard, P., Bjorkroth, J., 2016. Volatile organic compounds and *Photobacterium phosphoreum* associated with spoilage of modified-atmosphere-packaged raw pork. Int. J. Food Microbiol. 218, 86–95.

Nychas, G.J., Tassou, C.C., 1997. Spoilage processes and proteolysis in chicken as detected by HPLC. J. Sci. Food Agric. 74 (2), 199–208.

Nychas, G.-J.E., Skandamis, P.N., Tassou, C.C., Koutsoumanis, K.P., 2008. Meat spoilage during distribution. Meat Sci. 78 (1), 77–89.

Oakley, B.B., Morales, C.A., Line, J., Berrang, M.E., Meinersmann, R.J., Tillman, G.E., Wise, M.G., Siragusa, G.R., Hiett, K.L., Seal, B.S., 2013. The poultry-associated microbiome: network analysis and farm-to-fork characterizations. PLoS One 8 (2), e57190.

Pennacchia, C., Ercolini, D., Villani, F., 2011. Spoilage-related microbiota associated with chilled beef stored in air or vacuum pack. Food Microbiol. 28 (1), 84–93.

Polka, J., Rebecchi, A., Pisacane, V., Morelli, L., Puglisi, E., 2015. Bacterial diversity in

typical Italian salami at different ripening stages as revealed by high-throughput sequencing of 16S rRNA amplicons. Food Microbiol. 46, 342–356.
Proctor, L.M., Gunsalus, R.P., 2000. Anaerobic respiratory growth of *Vibrio harveyi, Vibrio fischeri* and *Photobacterium leiognathi* with trimethylamine N-oxide, nitrate and fumarate: ecological implications. Environ. Microbiol. 2 (4), 399–406.
Rossaint, S., Klausmann, S., Kreyenschmidt, J., 2015. Effect of high-oxygen and oxygen-free modified atmosphere packaging on the spoilage process of poultry breast fillets. Poult. Sci. 94 (1), 96–103.
Rouger, A., Tresse, O., Zagorec, M., 2017. Bacterial contaminants of poultry meat: sources, species, and dynamics. Microorganisms 5 (3).
Sáenz de Miera, L.E., Arroyo, P., de Luis Calabuig, E., Falagán, J., Ansola, G., 2014. High-throughput sequencing of 16S RNA genes of soil bacterial communities from a naturally occurring CO_2 gas vent. Int. J. Greenh. Gas Control. 29, 176–184.
Sante, V., Renerre, M., Lacourt, A., 1994. Effect of modified atmosphere packaging on color stability and on microbiology of turkey breast meat. J. Food Qual. 17 (3), 177–195.
Santos, M.S., 1996. Biogenic amines: their importance in foods. Int. J. Food Microbiol. 29 (2-3), 213–231.
Stoops, J., Ruyters, S., Busschaert, P., Spaepen, R., Verreth, C., Claes, J., Lievens, B., Van Campenhout, L., 2015. Bacterial community dynamics during cold storage of minced meat packaged under modified atmosphere and supplemented with different preservatives. Food Microbiol. 48, 192–199.
Usbeck, J.C., Kern, C.C., Vogel, R.F., Behr, J., 2013. Optimization of experimental and modelling parameters for the differentiation of beverage spoiling yeasts by Matrix-Assisted-Laser-Desorption/Ionization-Time-of-Flight Mass Spectrometry (MALDI-TOF MS) in response to varying growth conditions. Food Microbiol. 36 (2), 379–387.
Vihavainen, E.J., Björkroth, J., 2010. Microbial Ecology and Spoilage of Poultry Meat and Poultry Meat Products. Handbook of Poultry Science and Technology.
Wu, S., Zhu, Z., Fu, L., Niu, B., Li, W., 2011. WebMGA: a customizable web server for fast metagenomic sequence analysis. BMC Genomics 12 (1), 444.